Prominent electrochemical performance of Li₃VO₄/C-Ni anode via hierarchically porous architecture design

Jicheng Zhang,[a] Shibing Ni,*[a,b] Tao Kang,[a] Jun Tang,[a] Xuelin Yang*[a,b], Lulu Zhang[a,b]

[a]College of Materials and Chemical Engineering, Three Gorges University, 8 Daxue Road, Yichang, Hubei 443002, China.

[b]Hubei Provincial Collaborative Innovation Center for New Energy Microgrid, China Three Gorges University.

*E-mail: shibingni07@126.com.

Experimental section

Sample preparation

The chemicals were analytical grade and purchased from Shanghai Chemical Reagents. Ni foam (100 PPI pore size, 380 g m^{-2} surface density, 1.5 mm thick) was purchased from Changsha Lyrun New Material corporation. In a typical procedure, 1 mmol V_2O_5, 3 mmol Li_2CO_3 and 5 mmol hexamethylenetetramine were added in 30 ml distilled water. After stirring for 20 minutes, the homogeneous yellowy suspension was transferred into a 50 ml teflonlined autoclave, distilled water was subsequently added to 80% of its capacity. The autoclave was at last sealed and placed in an oven, heated at 120 °C for 24 h. The final transparent solution was transferred in a culture dish, 0.05 g citric acid was added in the solution. After stirring for 2h, Ni discs were immersed into the solution for 1h. After that, the Ni discs were dried and annealed in N_2 atmosphere at 500 °C for 5h. The weight of active Li_3VO_4/C on Ni disc can be estimated according to the weight difference between the Ni disc and the obtained Li_3VO_4/C-Ni ($m_{Li3VO4/C} = m_{Li3VO4/C-Ni} - m_{Ni}$).

Structure and morphology characterization

The structure and morphology of the resulting products were characterized by X-Ray powder diffraction (Rigaku Ultima IV Cu Kα radiation λ=1.5406 Å), field-emission scanning electron microscopy (FE-SEM JSM 7500F, JEOL), and transmission electron microscopy (TEM, FEI, Tecnai G2 F30) equipped with selected area electron diffraction (SAED).

Electrochemical characterization

For preparing anode, the as-prepared Li_3VO_4/C-Ni foam discs (diameter of 14 mm) were dried at 120 ^{o}C for 24 h in vacuum oven. 2025 coin-type half cells of Li/1 M $LiPF_6$ in ethylene carbonate, dimethyl carbonate and diethyl carbonate (EC/DMC/DEC, 1:1:1 v/v/v)/Li_3VO_4/C-Ni were assembled in an argon-filled dry box (MIKROUNA, Super 1220/750, H_2O<1.0 ppm, O_2<1.0 ppm). A Celgard 2400 microporous polypropylene was used as the separator membrane. For the fabrication of $LiFePO_4$ cathode, a mixture of commercial $LiFePO_4$, acetylene black, and polyvinylidene fluoride (PVDF) dissolved in N-methylpyrrolidine (NMP) solution (0.02 g mL^{-1}) with weight ratio of 7.5:1.5:1 were coated on aluminium foil and cut into disc electrodeswith a diameter of 14 mm. 2025 coin-type full cells with the $LiFePO_4$ cathode and the Li_3VO_4/C-Ni anode were assembled using the same technology of half cells. Considering the initial irreversible lithium ions consumption in charging, a capacity ratio of 1.2:1 between cathode and anode in full cells was adopted. Before the matching, half cell of $LiFePO_4$ cathode and Li_3VO_4/C-Ni was resembled and measured, respectively. Galvanostatic charge/discharge test was

characterized on a multichannel battery test system (LAND CT2001A) in the voltage region 0.02~3 V for half cells and 0.8~3.5 V for full cells. The cyclic voltammetry measurement of the electrodes (vs. Li^+/Li) was carried out on a CHI660C electrochemical workstation at a scan rate of 0.2 mV s^{-1} between 0 and 3 V. Electrochemical impedance spectroscopy measurements were performed on CHI660C electrochemical workstation under open circuit conditions over a frequency range from 0.01 Hz to 100 kHz by applying an AC signal of 5 mV in amplitude throughout the tests. Equivalent circuit fitting of EIS data was carried out via ZsimpWin software.

Tab. S1 The summarization of discharge capacity versus cycle number of various

Li_3VO_4 electrodes. (the references are in accordance with those in the manuscript).

| material	current (mA/g) 1C≈394 mA/g	reversible capacity mAh g^{-1}/cycle no.	ref.
Li_3VO_4	20 mA/g	283/25	1
Li_3VO_4/graphene	20 mA/g	378/50	2
Li_3VO_4/graphite	156 mA/g	468/100	3
Li_3VO_4/CNTs	2000 mA/g	250/2000	4
Li_3VO_4/C	0.8 C	363/40	5
Li_3VO_4/graphene	5 C	163/5000	6
Li_3VO_4/C	1 C	394/100	7
Li_3VO_4/graphene	0.2 C	453/200	8
Li_3VO_4/C	20 mA/g	245/50	9
Li_3VO_4/C	0.1 C	401/50	10
Li_3VO_4/C@EG	2000 mA/g	205/2000	11
	100 mA/g	405/200	
HP-Li_3VO_4/C	200 mA/g	381/300	12
	4000 mA/g	275/500	
Li_3VO_4/3DGNs	2000 mA/g	259/2500	19
Li_3VO_4	0.25 C	396/100	21
$Li_3VO_{4-δ}$	200 mA/g	286/200	23
Li_3VO_4	0.5 C	250/100	24
Li_3VO_4	1 C	190/100	25
Li_3VO_4	2000 mA/g	280/500	26
Li_3VO_4	0.1 C	311/50	27
Li_3VO_4/C-Ni	10 C	325/ 2000	this work
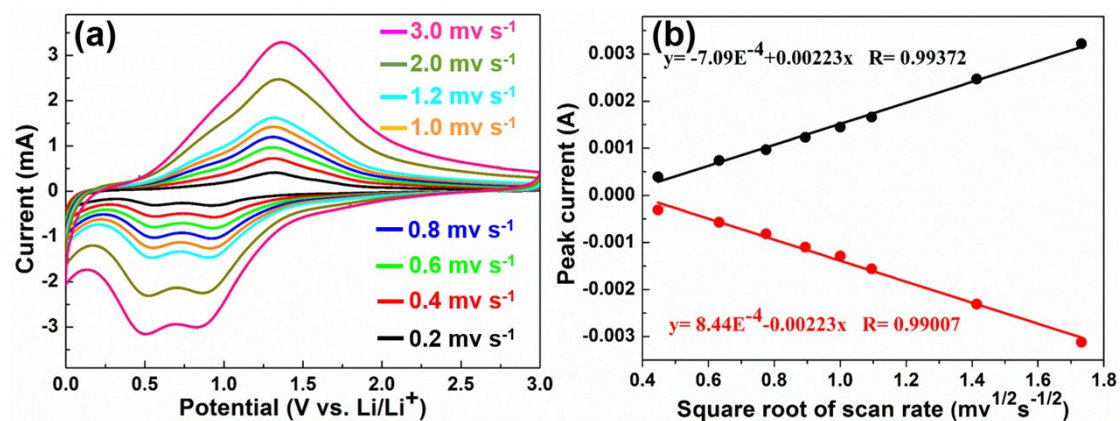
Fig. S1 (a) CV curves of the Li_3VO_4/C-Ni electrode at different scan rates between 0 and 3 V. (b) Dependence of peak current on the square root of the scan rate for the Li_3VO_4/C-Ni electrode.

CV curves of the Li_3VO_4/C-Ni electrode at scan rate from 0.2 to 3.0 mV s^{-1} are shown in Fig. S1(a). As seen, the reduction peaks shift to low potential regions with increasing scan rate, whereas the oxidation peak shifts to a high potential region, suggesting higher polarization under a high scan rate. Fig. S1(b) shows the relationship between peak current and the square root of the scan rate obtained from the experimental data in Fig. S1(a). As found, both the anodic and cathodic peak currents show a linear dependence on the square root of scan rate from 0.2 to 3 mV s^{-1}, suggesting a Li-ion diffusion controlled mechanism in the discharge and charge process [1]. High symmetry of the slope of the fitted lines indicates a highly reversible insertion and extraction of lithium ions in cycling.
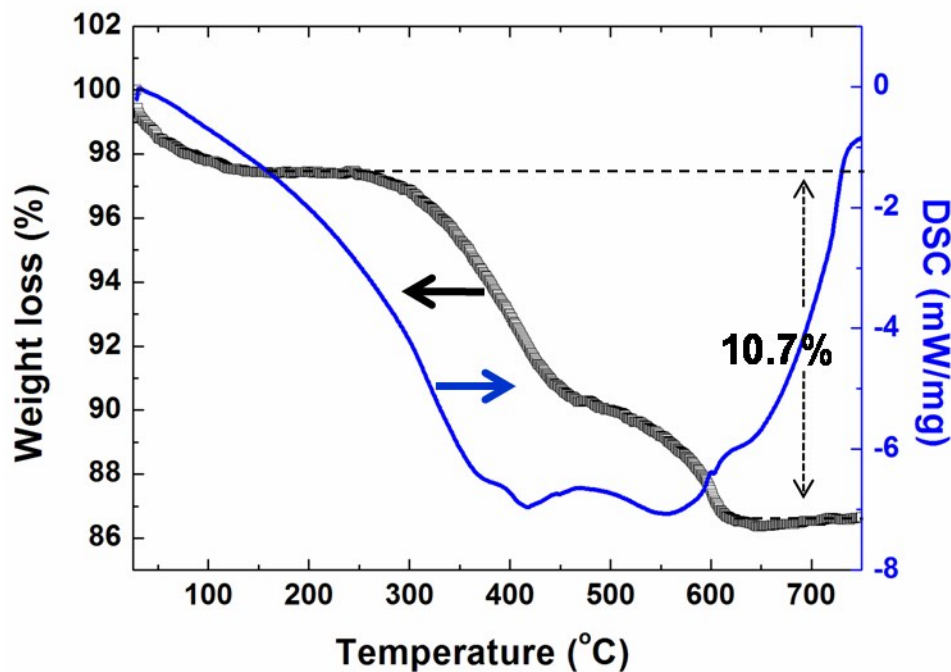
Fig. S2 TG and DSC curves of Li_3VO_4/C obtained under the same condition of Li_3VO_4/C-Ni electrode.

Fig. S2 shows the TG and DSC curves of the Li_3VO_4/C obtained under the same condition of Li_3VO_4/C-Ni electrode. The weight loss below 150 °C corresponds to the elimination of absorbed water, and the weight loss in temperature region 250~700 °C corresponds to the escape of C in Li_3VO_4/C. According to the TG results, the weight of C in Li_3VO_4 is about 10.7%. Considering the low specific capacity of amorphous C of about 300 mAh g^{-1}, the final specific capacity (~550 mAh g^{-1}) of the Li_3VO_4/C is resonable within the acceptable measuring error.

The morphology of the Li_3VO_4/C-Ni electrode after 2000 cycles is shown in Fig. S3. As seen, hierarchically porous characteristics of the electrode are kept, though the integral morphology of the electrode differs little from that before cycling. Such morphology variation originates from the reduction of particle-size of Li_3VO_4/C

owing to electrochemical activation and electrochemical reconstruction, which is similar to that in previous study [2].

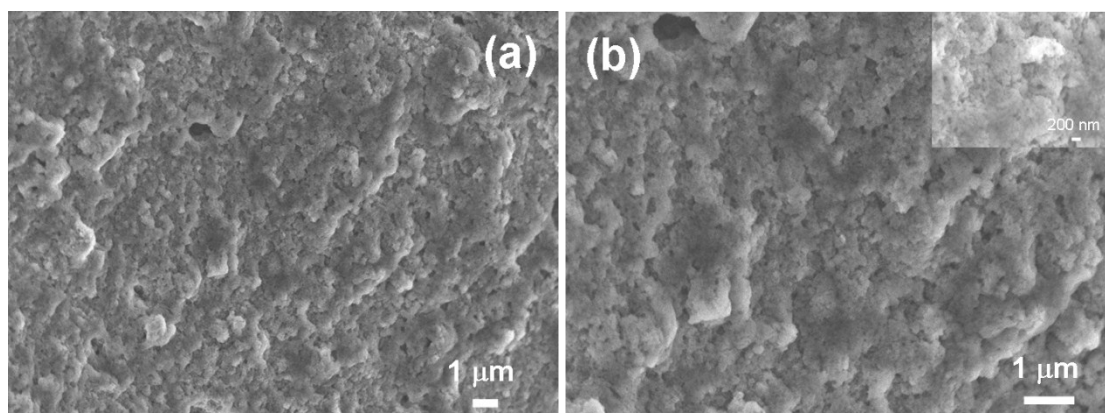Fig. S3 SEM images of the Li$_3$VO$_4$/C-Ni electrode after 2000 cycles with low (a) and high (b) magnification. The inset of (b) is a magnified SEM image.
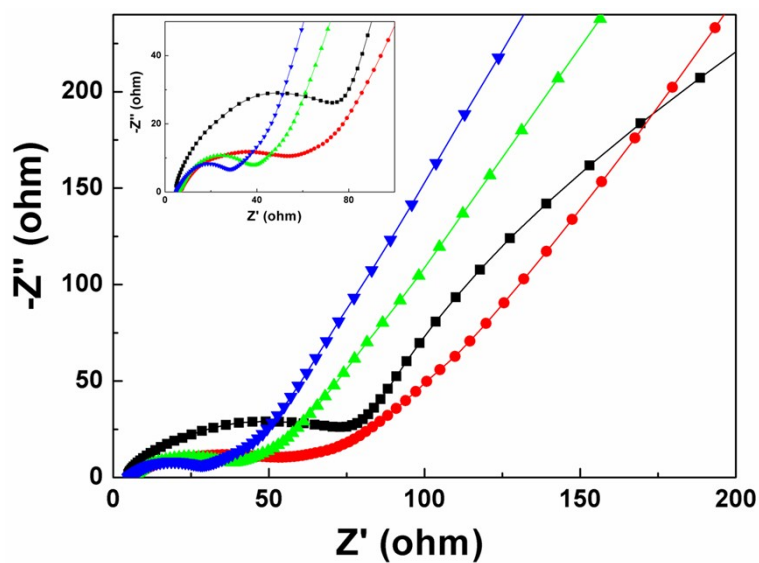

Fig. S4 AC impedance spectra of the Li$_3$VO$_4$/C-Ni electrode under different state. The inset shows the magnified part of the spectra.

Fig. S4 shows the electrochemical impedance spectra of the Li$_3$VO$_4$/C-Ni under different state. The intercept in high-frequency can be attributed to the contact resistance caused by SEI film and/or electrolyte, the medium-frequency semicircle is due to the charge-transfer impedance on electrode/electrolyte interface, and the

inclined line in low-frequency corresponds to the Li-ion diffusion process within electrodes [3]. The Nyquist plots were fitted via an R(C(RW)) equivalent circuit, and the contact and charge-transfer resistance of the electrode (Re and Rct) were obtained from the fitting results (Tab. S2). As seen, Re increases obviously after 2 cycles and then decreases along with the increasing of cycle number, which may be relevant to the gradual formation of stable SEI in the first few cycles. In addition, Rct for the Li_3VO_4/C-Ni decreases obviously along with the increasing of cycle number, suggest reduced charge transfer resistance. Such phenomena can ascribe to the originally high electronic conductivity based on the hierarchically porous architecture design and the unique electrochemical reconstruction in cycling that leads to enhanced contact between the integrate Li_3VO_4/C and the electric Ni foam substrate.

Tab. S2 Electrode kinetic parameters obtained from equivalent circuit fitting of Nyquist plots for Li_3VO_4/C-Ni electrode at different state.

Li_3VO_4/C-Ni	Re (Ω)	Rct (Ω)
fresh electrode	5.78	42.55
after 2 cycles	11.92	37.10
after 5 cycles	7.43	21.73
after 10 cycles	6.02	14.84

References

[1] Y. J. Zhu and C. S. Wang, *J. Phys. Chem. C*, 2011, **115**, 823-832.

[2] S. B. Ni, J. C. Zhang, J. J. Ma, X. L. Yang, L. L. Zhang, X. M. Li and H. B. Zeng, *Adv. Mater. Interfaces*, 2016, **3**, 1500340 10p.

[3] Z. Shi, J. Z. Wang, S. L. Chou, D. Wexler, H. J. Li, K. Ozawa, H. K. Liu and Y. P. Wu, *Nano Lett.*, 2013, **13**, 4715-4720.